# Structural characterization of environmentally relevant ternary uranyl citrate complexes present in aqueous solutions and solid state materials.

Madeline Basile, Daniel K. Unruh, Erin Flores, Adam Johns, and Tori Z. Forbes*
*Department of Chemistry, University of Iowa, Iowa City, IA 52242, USA*

*corresponding author; Email: tori-forbes@uiowa.edu

## Abstract

Organic acids are important metal chelators in environmental systems and tend to form soluble complexes in aqueous solutions, ultimately influencing the transport and bioavailability of contaminants in surface and subsurface waters.   This is particularly true for the formation of uranyl citrate complexes, which have been utilized in advanced photo- and bioremediation strategies for soils contaminated with nuclear materials.  Given the complexity of environmental systems, the formation of ternary or heterometallic uranyl species in aqueous solutions are also expected, particularly with Al(III) and Fe(III) cations.  These ternary forms are reported to be more stable in aqueous solutions, potentially enhancing contaminant mobility and uptake by organisms, but the exact coordination geometries of these soluble molecular complexes have not been elucidated.  To provide insight into the nature of these species, we have developed a series of geochemical model compounds   ($[(UO_2)_2Al_2(C_6H_4O_7)_4]^{6-}$ (**$U_2Al_2$**), $[(UO_2)_2Fe_2(C_6H_4O_7)_4]^{6-}$ (**$U_2Fe_2$-1**) and $[(UO_2)_2Fe_2(C_6H_4O_7)_4(H_2O)_2]^{6-}$ (**$U_2Fe_2$-2**) and $[(UO_2)_2Fe_4(OH)_4(C_6H_4O_7)_4]^{8-}$ (**$U_2Fe_4$**)) that were characterized by single-crystal X-ray diffraction and vibrational spectroscopy. Mass spectroscopy was then employed to compare the model compounds to species present in aqueous solutions to provide an enhanced understanding of the ternary uranyl citrate complexes that could be relevant in natural systems.

## Introduction

Citrate $(C_5H_5O(COO)_3)^{3-}$ is a naturally occurring polycarboxylate anion that plays an important role in the mobility and bioavailability of metals in aqueous environmental systems. A significant amount of the citrate found in natural systems is formed through biomass decay or produced by the plant roots or microorganisms.[1] Extrusion of citrate by plant roots increases solubility and enhances uptake of essential trace elements, such as Fe(III) or P (in the molecular form of orthophosphate), but can be also be a strategy of ameliorating heavy metal and Al toxicity.[2-4] Citrate concentrations in bulk soil is estimated to be <50uM, but can be concentrated in the rhizosphere at levels between 5-50 μmol/g soil.[3-5] Due to the ability of the citrate ligand to solubilize a wide range of metal cations and oxyanions, it has also been utilized as a soil amendment to mobilize contaminants for "pump-and-treat" remediation strategies.[6, 7]

Hexavalent uranium is one such radioactive, heavy metal contaminant that can be impacted by the presence of citrate in subsurface environments.[8] Uranium is a naturally occurring radioactive element that is primarily utilized as a fuel source for nuclear power.[9, 10] The mining and milling of uranium and the historical production of transuranic materials for nuclear weapons comprises the major sources for environmental contamination.[11, 12] Under aerobic conditions, uranium exists in the hexavalent state and forms two strong bonds to O atoms to create a nearly linear-dioxo cation, $U(VI)O_2^{2+}$.[13] This uranyl cation can form carbonate complexes in solution, undergo hydrolysis to form polynuclear species, or precipitate as uranyl mineral phases depending on the aqueous environmental conditions. Under slightly acidic conditions, citrate will complex to the uranyl cation through the equatorial plane in a polydentate fashion, forming a mononuclear species.[14, 15] As the pH increases, hydrolysis of the metal center can take place, forming dimers, trimers, and other polynuclear species.[14, 16, 17] The presence of

citrate in the environment has been linked to enhanced mobility of $U(VI)O_2^{2+}$ as Eps et al, have observed more than a 365-fold increase in the solubility of $U(VI)O_2^{2+}$ when citric acid was added as an amendment.[18]    In addition, the inclusion of citrate during the phytoremediation of $U(VI)O_2^{2+}$ from contaminated soils increased the accumulation and uptake by a factor of 14.[19] These previously reported studies suggest that the presence of the citrate ligand will have a profound effect on the bioavailability and mobility of $UO_2^{2+}$ in subsurface environments.

While the formation of uranyl citrate species in subsurface environments is relatively well understood, the presence of other metals in soil systems adds an additional level of complexity to the system.[14, 16, 17] Trivalent iron and aluminum are abundant in soils, occurring as solid bulk and nanomineral phases, more mobile colloids, or solubilized organic chelates, such as those observed for citrate (cit) complexes. Mononuclear forms, including $[M(cit)_2]^{5-}$, $[M(Hcit)_2]^{4-}$, and $[M(Hcit)_2]^{3-}$ (M = Al(III), Fe(III)), have been observed in slightly acidic pH regions, whereas polynuclear complexes ($[M_2OH_x(cit)_2]^{y-}$) form under more neutral conditions.[20-22] Given the ability of citrate to bind to an array of metal cations, ternary or heterometallic species are also likely to form and 1:1:2 $U(VI)O_2^{2+}$:Fe(III):citrate complexes have been observed previously in aqueous systems.[23] Formation of ternary molecular species could impact the long term stability of $U(VI)O_2^{2+}$-bearing mineral due to higher solubility of the resultant phases and several previous studies have reported enhanced mobility and stability in mixed-metal systems. [23-26] Other studies hypothesize that contaminant mobility will decrease when excess citrate binds to the surface of Fe(III) and Al(III) oxide mineral surfaces, providing enhanced adsorption and retention.[26, 27] While the fate and transport of $U(VI)O_2^{2+}$/(Fe(III), Al(III))/citrate complexes in environmental systems is unclear, the previously reported data demonstrates the importance of these ternary phases. [26, 27]

Despite the impact of these species in solution, only a handful of studies investigating ternary $U(VI)O_2^{2+}$:(Fe(III), Al(III)):citrate complexes have been previously reported in the literature and very few contain the structural characteristics of the resultant phases.[28, 29] Developing a complete picture of the ternary species present in solution is difficult given the complexity of the system and the multitude of possible polynuclear phases that are difficult to discern using potentiometric and spectroscopic approaches. We are interested in providing a deeper understanding of the formation of ternary phases for actinides in aqueous conditions through the structural characterization of geochemical model compounds. These models are created through the crystallization of the molecular species into an extended 3-D lattice through charge balancing cations, which allows for the structural characteristics of the species to be determined using single-crystal X-ray diffraction. This solid compound can then be chemically characterized by a variety of techniques, which provides foundational knowledge that can be applied to aqueous solution studies. Herein, we present the synthesis and chemical characterization of three novel ternary molecular species: $[(UO_2)_2Al_2(C_6H_4O_7)_4]^{6-}$ (**$U_2Al_2$**), $[(UO_2)_2Fe_2(C_6H_4O_7)_4]^{6-}$ (**$U_2Fe_2$**), and $[(UO_2)_2Fe_4(OH)_4(C_6H_4O_7)_4]^{8-}$ (**$U_2Fe_4$**). These solid phases were compared to previously reported speciation studies to provide additional insight into the formation of ternary phases in environmentally relevant aqueous solutions.

## Results and Discussion

*Structural Descriptions*

### $[(UO_2)_2Al_2(C_6H_4O_7)_4]^{6-}$ (**$U_2Al_2$**).

A ternary molecule with a $U(VI)O_2^{2+}$:Al(III):citrate ratio of 2:2:4 is observed in the **$U_2Al_2$** species (Fig. 1). The average bond length between the U(VI) metal center and the axial O

atoms was 1.767(4) Å, which is typically observed for the near linear uranyl $U(VI)O_2^{2+}$ cation.

Six additional equatorial bonds with distances ranging from 2.341(5) – 2.581(5) Å result in the

formation of a hexagonal bipyramidal coordination geometry about the U(VI) cation.   Each

Al(III) cation is octahedrally coordinated by six ligands with distances ranging from 1.821(5) to

1.905(3) Å.   The citrate molecule contains three carboxylate functional groups and one central

hydroxyl group that allows the chelator to form up to four bonds with a metal center.   In the case

of the **U₂Al₂** species, two citrate molecules bridge one uranyl polyhedron and one Al(III)

octahedron through the central hydroxyl functional group.   In addition, each of the citrate

molecules bond to the Al(III) cation through two carboxylate functional groups, leaving one arm

available to complex to the U(VI) atom, resulting in the 1:1:2 $U(VI)O_2^{2+}$:Al(III):Cit species. Two

of these building units self-assemble to form the 2:2:4 species, with the central $U(VI)O_2^{2+}$ dimer

created through bridging O atoms of with the carboxylate functional groups and the two Al

octahedra decorating the exterior of the molecule.  Overall, the cluster is negatively charged with

a molecular formula of $[(UO_2)_2Al_2(C_6H_4O_7)_4]^{6-}$.

The $[(UO_2)_2Al_2(C_6H_4O_7)_4]^{6-}$ species can be crystallized into two separate compounds,

**U₂Al₂-1** and **U₂Al₂ -2**, due to the presence of different charge balancing cations within the

crystalline lattice that lead to changes in molecular packing and unit cell dimensions.  For **U₂Al₂-**

**1**, the negative charge on the cluster is balanced by three piperazinium cations, while the

presence of two strontium and one ethylenediamonium cations results in a different crystalline

packing for **U₂Al₂-2**.  Additional interstitial water molecules participate in hydrogen bonding

interactions and are located throughout the crystalline lattice void spaces in both compounds.

The amount of water present in the crystalline lattice was verified by TGA, leading to the overall

chemical formulas of $[(C_4H_{12}N_2)_3][(UO_2)_2Al_2(C_6H_4O_7)_4](H_2O)_8$ and

$[Sr_2(C_2H_{10}N_2)][(UO_2)_2Al_2(C_6H_4O_7)_4](H_2O)_{13}$ for **U₂Al₂-1** and **U₂Al₂-2**, respectively.

## $[(UO_2)_2Fe_2(C_6H_4O_7)_4]^{6-}$ and $[(UO_2)_2Fe_2(C_6H_4O_7)_4(H_2O)_2]^{6-}$ (U₂Fe₂-1 and U₂Fe₂-2)

The heterometallic cluster found in **U₂Fe₂-1** is isostructural to the $U(VI)O_2^{2+}$/Al(III)

tetramer, but **U₂Fe₂-2** exhibits a slight variation in the chelation of Fe(III) metal center by the

citrate molecule (Fig. 2). Two central U(VI) hexagonal bipyramids are again observed with

average $U-O_{ax}$ and $U-O_{eq}$ (ax = axial, eq = equatorial) bond lengths of 1.764(4) and 2.478(4) Å,

respectively. Each of the two Fe(III) octahedra are bonded to the exterior of the uranyl dimer

through a bridging hydroxo group, with Fe-O bond lengths ranging from 1.935(4) to 2.058(4) Å.

While chelation of the U(VI) polyhedra by the citrate ligand is identical to the ternary

$U(VI)O_2^{2+}$/Al(III) citrate species in both complexes, a slight variation is observed for the Fe(III)

metal centers. Tetradentate chelation of the Fe(III) cation in **U₂Fe₂-1** occurs via two of the citrate

carboxylate O atoms, one shared O atom between the two metal cations, and an O atom

associated with the uranyl cation. In the case of **U₂Fe₂-2**, tridentate chelation is observed

because one arm of the citrate ligand is not complexed to the metal center, leading to the

presence of an additional water molecule bound to the Fe(III) cation. In both species, the overall

charge on the cluster is negative six, but the molecular formula is $[(UO_2)_2Fe_2(C_6H_4O_7)_4]^{6-}$ and

$[(UO_2)_2Fe_2(C_6H_4O_7)_4(H_2O)_2]^{6-}$ for **U₂Fe₂-1** and **U₂Fe₂-2**, respectively.

Differences in the crystalline packing for **U₂Fe₂-1** and **U₂Fe₂-2** can also be observed due

to the identity of the charge balancing cations present in the reaction vial. The negative six

charge associated with the cluster in **U₂Fe₂-2** is balanced by three doubly deprotonated

piperazinium cations, while the **U₂Fe₂-1** cluster is balanced by two piperazinium cations and a

hydrated magnesium cation. Water molecules again occupy the interstitial regions of the

compounds and partake in hydrogen bonding interactions between the core cluster units, which results in the crystallization of the neutral $[Mg(H_2O)_4(C_4H_{12}N_2)_2][(UO_2)_2Fe_2(C_6H_6O_7)_4](H_2O)_7$ and $[(C_4H_{12}N_2)_3][(UO_2)_2Fe_2(C_6H_4O_7)_4(H_2O)_2](H_2O)_2$ for **U₂Fe₂-1** and **U₂Fe₂-2**, respectively.

## $[(UO_2)_2Fe_4(C_6H_4O_7)_4O_2(OH)_4]^{8-}$ (U₂Fe₄)
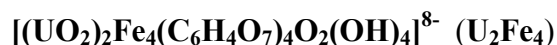
A slightly larger ternary complex with a U:Fe:citrate ratio of 2:4:4 is observed in the **U₂Fe₄** compound (Fig. 3). Each uranyl cation is surrounded by five ligands, resulting in a pentagonal bipyramidal geometry with average $U(VI)-O_{ax}$ and $U(VI)-O_{eq}$ bonds of 1.791(5) and 2.359(5) Å, respectively. The Fe(III) cation is coordinated by six ligands in an octahedral coordination with bond distances ranging from 1.855(5) to 2.119(5) Å. Two $\mu_2$-OH bridged Fe(III) dimers are further bonded through $\mu_3$-O atoms, forming a tetrameric Fe₄ unit that comprises the core of the **U₂Fe₄** ternary species. Each uranyl polyhedra is bonded to the central molecular unit via the $\mu_3$-O atom and through the bridging hydroxyl functional group of the citrate ligand to create a U:Fe ratio of 2:4. Four citrate molecules bridge the $U(VI)O_2^{2+}$ and Fe(III) polyhedra, completing the inner sphere coordination shell for both metals. The molecular cluster of the **U₂Fe₄** compound has a negative eight charge that is balanced out by four ethylenediammonium cations. These ancillary cations plus fourteen water molecules per cluster, are located within the interstitial regions and aid in linking the **U₂Fe₄** clusters into a 3-D crystalline lattice. The overall formula for the neutral, heterometallic compound **U₂Fe₄** is $[(C_2H_{10}N_2)_4][(UO_2)_2Fe_4(C_6H_4O_7)_4O_2(OH)_4](H_2O)_{14}$.

*Vibrational Spectroscopy*

Fourier transform infrared spectroscopy of the **U₂Fe₄, U₂Fe₂,** and **U₂Al₂** compounds confirms the citrate complexation of the metal center and the presence of solvated and ligated

water (Fig. 4). All spectra contain a strong vibrational mode at 925 cm$^{-1}$ that corresponds to the $v_3$ asymmetric stretch of the uranyl cation.[30] Bands present at 1390 cm$^{-1}$ and 1600 cm$^{-1}$ correlate to the asymmetric and symmetric stretching modes associated with the –COO$^-$ functional group of the citrate molecule, respectively.[14, 31] Several O-H stretching vibrations from free solvent molecules, ligated water groups, and the bridging hydroxyl groups were observed as a broad peak ranging from 2900 to 3650 cm$^{-1}$.[30] The bending mode associated with the solvent water molecules can also be observed at approximately 1640 cm$^{-1}$, but overlaps with the asymmetric stretching band of the –COO$^-$ functional group.[32] Additional weak peaks related to C-H vibrational modes are present between 400-1600 cm$^{-1}$.

The $v_1$ symmetry stretching vibration associated with the uranyl cation dominates the Raman spectra for all three complexes and can be utilized to provide some information regarding bond strength (Fig. 5). This band is observed at 835 cm$^{-1}$ for both **U$_2$Al$_2$** and **U$_2$Fe$_2$** and is red shifted compared to the aqueous pentaaqua uranyl species that was previously reported at 870 cm$^{-1}$. A decrease of 30-60 cm$^{-1}$ from the solvated uranyl cations is common for species that are complexed by electron donating ligands, such as carboxylate and hydroxyl functional groups.[33, 34] The $v_1$ band is observed at 813 cm$^{-1}$ for **U$_2$Fe$_4$** complex and the additional red shift may be explained by the presence of the bridging $\mu_3$-O in the molecule that will provide additional electron donation and elongation of the uranyl bond. Due to the observed changes in the Raman spectra for the **U$_2$Fe$_2$** and the **U$_2$Fe$_4$** species, the position of the $v_1$ symmetry stretch may be utilized to identify ternary species in solution.

*Mass Spectrometry*

Electrospray ionization mass spectrometry (ESI-MS) verifies the presence of stable anionic species in solution and can be related to the ternary species characterized in the solid state by single-crystal X-ray diffraction. The soft ionization of an electrospray source has the ability to transfer material into the gas phase relatively intact which makes ESI-MS a desirable technique for the characterization of aqueous ionic species with high molecular weights.[14, 35, 36] Fragmentation of the molecular species occurs quite readily for these complexes; therefore, it is important to investigate the anionic species associated with **U$_2$Fe$_4$, U$_2$Fe$_2$,** and **U$_2$Al$_2$** compounds that can be observed with ESI-MS.

To investigate the stability of the ternary species under a variety of aqueous conditions, the solid material was redissolved in water with the pH adjusted between 4 and 10 with a NH$_4$OH buffer. This provides a solution that contains just one molecular cluster instead of a range of polynuclear species, which provides exact information on the fragmentation that occurs during the ESI-MS measurement. These initial studies provide the basis for understanding environmentally relevant solution that contain a multitude of molecular species, charge balancing cation/anions, or other organic matter. In all cases, the 2:2:4 U:Fe, Al:Cit or the 2:4:4 U:Fe:Cit molecule were not observed as the major species. Instead, the species that was detected corresponded to $[UO_2 -(Fe,Al)- 2Cit + H]^{2-}$ with an *m/z* = 351 for **U$_2$Fe$_2$** and **U$_2$Fe$_4$** and 337 for **U$_2$Al$_2$**. This 1:1:2 U:(Fe, Al):Cit anionic species is dominant at pH values greater than 6, with only a handful of minor fragments observed with relative abundance <15. The molecular species associated with these minor peaks were not identified, but suggests additional fragmentation to mononuclear and binuclear species. Full spectra of the solutions at pH 8-9 are available in the supporting information section and are representative of all solutions.

*Relationships to aqueous solutions*

The objective of the current study is to structurally characterize ternary molecular species to use as geochemical model compounds and provide additional chemical characterization to serve as foundational knowledge for the identification of these species in aqueous conditions. An important point regarding crystallization is that the species isolated in the solid-state may not represent the major species in solution, but instead is preferentially crystallized based on the identity of the charge balancing cation or other spectator ions present in solution. Due to this fact, it is necessary to compare the data collected on the molecular species present in the solid-state lattice to studies performed on aqueous systems. As a slight extension, structural information for the first and second coordination sphere of the metals can also be useful for the adsorption of contaminants on mineral surfaces. In the current section, we compare the structural details of the **U₂Al₂**, **U₂Fe₂**, and **U₂Fe₄** complexes to previously reported data on related systems.

Under acidic conditions, U(VI) speciation is dominated by the pentaaquauranyl complex, $[(UO_2)(H_2O)_5]^{2+}$, but upon increasing pH hydrolysis of the metal center can occur, which results in the formation of larger polynuclear molecules.[37] Hydrolysis can occur via two pathways, olation and oxolation, where the former generally occurs by the elimination of a water molecule and the formation of hydroxo bridges.[38, 39] Oxolation ensues when a hydroxo or oxohydroxo complex is initially formed and water molecule is not available as a leaving group, resulting in condensation that proceeds via deprotonation of a hydroxo group to form a oxo bridge.[38, 39] Hydrolysis of the uranyl cation in aqueous solution generally occurs when the pH > 3 with an olation reaction resulting in the formation of the dimeric $[(UO_2)_2(\mu_2\text{-}OH)_2(H_2O)_6]^{2+}$ species.[40-42] This species is never observed as the sole soluble complex because it is in thermodynamic

equilibrium with monomeric $U(VI)O_2^{2+}$ and $(U(VI)O_2)(OH)^+$ forms.[40]   Increasing alkalinity results in the creation of trimeric species that have previously been identified as $[(UO_2)_3(OH)_4]^{2+}$ and $[(UO_2)_3(OH)_5]^+$ by potentiometric studies.[40, 42]   Several uranyl trimer have been crystallized into the solid phase and structurally characterized by single-crystal X-ray diffraction.[43-46]   In near-neutral aqueous solutions, the trimeric species that is generally observed contains a central $\mu_3$-O and three $\mu_2$-OH bridges and this form has been reported as the most thermodynamically stable phase based upon DFT studies.[47]

Addition of complexing agents, such as citrate, can influence the speciation and structural characteristics of the resulting hydrolysis products.[46, 48]   In binary systems, uranyl citrate dimers begin to coalesce at a pH of approximately three and the proposed structure based on NMR studies suggests that the uranyl moieties are bridged by the α-hydroxy groups on two separate citrate ligands result in a molecule with a $U(VI)O_2^{2+}$:citrate ratio of 2:2.[14, 17, 49, 50] Given the steric hindrance, it is postulated that only two of the carboxylate functional groups associated with a citrate molecule are chelated to the metal centers, leaving one arm uncomplexed.[49]   This arrangement of the citrate would result in a square bipyramidal coordination about the metal center, although it is possible that an additional water molecules could be present to form the more widely observed pentagonal bipyramidal geometry.   Under slightly acidic to neutral conditions, a trimeric species is expected as the dominate form, but two different species with variations in the $U(VI)O_2^{2+}$:citrate ratio (3:3 and 3:2) have been previously observed in solution.[14]   The structural characteristics of the 3:3 U:cit species have yet to be determined through any means, although it is postulated that a ring structure exists for the 3:2 U:cit molecule.[17]

Fe(III) and Al(III) are also susceptible to hydrolysis in aqueous conditions and can form large polyncuclear species with cubane-type structures, such as the, $Fe_7$, $Fe_9$, $Fe_{11}$, $Fe_{13}$, $Fe_{17}$, and $Fe_{19}$ molecular complexes.[51-55] Hydrolysis of the Fe(III) cation also takes place through olation reactions with the formation of $\mu_2$-OH bridging the metal centers.[39] Under acidic conditions and in the presence of citrate, dimeric Fe(III) can form with Fe:citrate ratios of 2:2 or 2:3.[56] In both species, the Fe(III) metal centers are bridged through the hydroxyl functional groups of the citrate, which is similar to that observed for the uranyl dimeric complex. Trimeric Fe(III) citrates have also been reported with a "voided cubane" core that link together through the carboxylate end members, forming a nonairon (III) citrate complex or the "ferric triple-decker".[57] Aluminum citrate speciation is very similar to Fe(III), however no large polynuclear species have been structurally characterized.[21, 58]

Formation of heterometallic or ternary species containing $U(VI)O_2^{2+}$ and Fe(III) or Al(III) hydrolysis products are likely to occur in environmental systems, given the ability of the citrate ligand to complex all three metal cations. An Al(III)- $U(VI)O_2^{2+}$ complex has previously been detected using amperometric and spectrophotometric techniques that indicated the presence of a central U atom was bonded to two citrate molecules and an Al(III) cation is likely bound to O atoms associated with the uranyl polyhedra.[23] Ternary $Fe(III)/U(VI)O_2^{2+}$ species have previously been reported by several studies and initial characterization of the complex suggested a binuclear iron core coordinated in a bidentate fashion to two complexed uranyl polyhedra through the central carboxylate functional group of the citrate.[24, 28, 29]

Additional structural studies conducted on solutions and solid phases with $U(VI)O_2^{2+}$:Fe(III):Cit ratio of 1:1:2 was previously performed by Dodge and Francis[28] using Extended X-ray Absorption Fine Structure (EXAFS) Spectroscopy. Bond lengths based upon

single-crystal X-ray diffraction of the compounds reported herein and the reported EXAFS data[28] for the ternary iron-uranyl citrate complexes are summarized in Table 1. Distinct differences in the bond lengths are observed between the two structural characterization techniques, suggesting the formation of very different complexes. EXAFS data of the solution phase indicated that a Fe(III) dimer was the central core of the molecular species, which is opposite to that observed in $Fe_2U_2$. A tetrameric iron core is observed for the $Fe_4U_2$ species, but there are differences in the atom-atom distances between the metal centers. The EXAFS data provides Fe(III)-Fe(III) distances of 3.74 and 3.61 Å for the solid phase and 15mM solution, respectively, whereas the X-ray diffraction data observed distances at 3.073 Å for the $\mu_2$-OH bridged Fe(III) dimers and 3.602 Å and for the $\mu_3$-O bridging mode. A peak was observed in the Fourier Transform of the EXAFS data at 3.02 Å, but it was assigned to the Fe(III)-C distance. Additional discrepancies between the data includes an unexplained distance at 2.72 Å from the Fe(III) cation in the EXAFS spectra. Both the solution and the solid phase material contained $Na^+$ cations due to the addition of NaOH and thus Dodge and Francis[28] assigned this peak to a Fe-Na distance. The $U(VI)O_2^{2+}$:Fe(III):citrate species presented in this work do not contain additional $Na^+$ cations, thus this distance could not be confirmed.

The importance of understanding the structural details of these complexes is highlighted by studies that indicate the ternary 1:1:2 $U(IV)O_2^{2+}$:Fe(III):Cit are resistant to biodegradation in aqueous solutions. Photo- and biodegradation of these soluble complexes has been identified as a potential pathway to the environmental remediation of uranium thus it is important to understand the impact of ternary complexes present in solution. Dodge and Francis[29] previously reported that these mixed metal species are completely recalcitrant to biodegradation by *Pseudomons fluorescens*, whereas the 1:1 Fe(III):Cit and $U(VI)O_2^{2+}$:Cit complexes readily

degrade. Additional investigations by Francis et al.[59] on a range of metal citrate complexes suggested that the complexation of the alcohol group to the metal center results in the resistance to degradation. The complex formed in **U₂Fe₂**, as well as those observed in **U₂Al₂** and **U₂Fe₄**, contain complexed alcohol groups, suggesting that these species will also exhibit a resistance to biodegradation by microbes.

## Conclusions

Four ternary $U(VI)O_2^{2+}$:(Fe(III),Al(III)):Cit complexes were structurally and chemically characterized to provide an enhanced understanding of the formation of molecular species in heterometallic aqueous systems. While discrepancies exist between the single-crystal X-ray diffraction data and the results from the EXAFS data, the ability to compare atomic distances, is crucial for providing structural understanding of the species observed in aqueous systems. In addition, spectroscopic studies of solid state materials provide an ideal model complex that can be utilized to predict the expected vibrational bands in aqueous solution and can aid in the identification of the molecular fractionation that are observed in mass spectrometry. Further characterization of molecular heterometallic $U(VI)O_2^{2+}$/(Fe(III), Al(III)) structures is important for providing a complete picture of speciation in aqueous solutions and leading to advancements in remediation strategies and transport modeling of actinides in environmental systems.

## Experimental Section

**Synthesis.** $UO_2(NO_3)_2 \cdot 6H_2O$ was purchased from Flynn Scientific Inc., $Fe(NO_3)_3 \cdot 9H_2O$ from Alfa Aesar, $Al(NO_3)_2 \cdot 9H_2O$ from Acros Organic, and $C_6H_8O_7 \cdot H_2O$ from J.T. Baker. All chemicals were reagent grade and used without further purification.

**[(C$_4$H$_{12}$N$_2$)$_3$][(UO$_2$)$_2$Al$_2$(C$_6$H$_4$O$_7$)$_4$](H$_2$O)$_8$: U$_2$Al$_2$-1** was obtained by the combination of 2 mL of 0.2 M aqueous uranyl nitrate hexahydrate (0.4 mmol), 2 mL of 0.2 M aqueous aluminum nitrate nonahydrate (0.4 mmol) and 4 mL of 0.2 M aqueous citric acid monohydrate (0.8 mmol) in a 20 mL glass scintillation vial.  The pH of the resulting solution was increased to 4.1 with 0.8 M aqueous piperazine hexahydrate and **U$_2$Al$_2$-1** was crystallized out by a liquid-liquid diffusion method with acetonitrile (1:2 solution:solvent) in low (>5%) yield.

**[Sr$_2$(C$_2$H$_{10}$N$_2$)][(UO$_2$)$_2$Al$_2$(C$_6$H$_4$O$_7$)$_4$](H$_2$O)$_{13}$: U$_2$Al$_2$-2** was obtained by the combination of 2 mL of 0.2 M aqueous uranyl nitrate hexahydrate (0.4 mmol), 2 mL of 0.2 M aqueous aluminum nitrate nonahydrate (0.4 mmol) and 4 mL of 0.2 M aqueous citric acid monohydrate (0.8 mmol) in a 20 mL glass scintillation vial.  The pH of the resulting solution was increased to 4.0 with 20 v/v% aqueous ethylenediamine and then 0.235 mL of 0.2 M aqueous Sr(NO$_3$)$_2$ (11.1 µmol) was incorporated into the reaction solution.  **U$_2$Al$_2$-2** was crystallized out by liquid-liquid method diffusion with acetonitrile (1:2 solution:solvent) in 72% yield.

**[(Mg(H$_2$O)$_4$)(C$_4$H$_{12}$N$_2$)$_2$][(UO$_2$)$_2$Fe$_2$(C$_6$H$_4$O$_7$)$_4$](H$_2$O)$_7$:  U$_2$Fe$_2$-1** was obtained by the combination of 2 mL of 0.2 M aqueous uranyl nitrate hexahydrate (0.4 mmol), 2 mL of 0.2 M aqueous ferric nitrate nonahydrate (0.4 mmol) and 4 mL of 0.2 M aqueous citric acid monohydrate (0.8 mmol) in a 20 mL glass scintillation vial.  The pH of the resulting solution was increased to 4.0 with 0.8 M aqueous piperazine hexahydrate and then 0.235 mL of 0.2M aqueous Mg(NO$_3$)$_2$·6H$_2$O (11.1 µmol) was incorporated into the reaction solution.  **U$_2$Fe$_2$-1** was crystallized out by liquid-liquid diffusion with acetonitrile (1:1 solution:solvent) in 80% yield.

**[(C₄H₁₂N₂)₃][(UO₂)₂Fe₂(C₆H₄O₇)₄(H₂O)₂](H₂O)₂: U₂Fe₂-2** was obtained by the combination of 2 mL of 0.2 M aqueous uranyl nitrate hexahydrate (0.4 mmol), 2 mL of 0.2 M aqueous ferric nitrate nonahydrate (0.4 mmol) and 4 mL of 0.2 M aqueous citric acid monohydrate (0.8 mmol) in a 20 mL glass scintillation vial.  The pH of the resulting solution was increased to 4.0 with 0.8 M aqueous piperazine hexahydrate and **U₂Fe₂-2** was crystallized out by liquid-liquid diffusion with acetonitrile (1:1 solution:solvent) in low (>5%) yield.

**[(C₂H₁₀N₂)₄][(UO₂)₂Fe₄(C₆H₄O₇)₄O₂(OH)₄](H₂O)₁₄: U₂Fe₄** was obtained by the combination of 2 mL of 0.2 M aqueous uranyl nitrate hexahydrate (0.4 mmol), 2 mL of 0.2 M aqueous ferric nitrate nonahydrate (0.4 mmol) and 4 mL of 0.2 M aqueous citric acid monohydrate (0.8 mmol) in a 20 mL glass scintillation vial.  The pH of the resulting solution was increased to 7.0 with 20 v/v% aqueous ethylenediamine and **U₂Fe₄** was crystallized out by liquid-liquid diffusion with tetrahydrofuran (1:4 solution:solvent) in 86% yields.

**Single-Crystal X-ray Diffractometry.**  The crystalline data acquisition for all five complexes were collected on a Nonius Kappa CCD single-crystal X-ray diffractometer equipped with graphite-monochromated Mo Kα radiation (λ = 0.7107 Å) and a low-temperature cryostat set at 100 K.  The Nonius COLLECT software[60] acquired the data and the Bruker APEX II software performed the Lorentzian, polarization, data integration and background correction on the collected data.[61]  A semi-empirical correction for crystal absorption was completed using the SADABS program within the APEX II software[61] and all crystal structures were determined by direct methods and refined on the basis of $F^2$ for all unique data using the Bruker SHELXTL version 5.01 software.[62]  The U, Al, Fe, Sr, and Mg atoms were determined in the intial structure

solution and the O, C, and N atoms were identified in the difference Fourier maps calculated following refinement of the partial structure models.  Hydrogen atoms associated with the organic componense were constrained using a riding model.  When ordered water molecules were present in the interstitial regions, H atoms were identified electron density and placed using the DFIX restraints.  H atoms were not placed on disordered water molecules. Selected data collection parameters and crystallographic information are provided in Table 2. Crystallographic information files (CIFs) for each compound are available free of charge at the Cambridge Crystallographic Data Centre upon providing reference numbers 1018644-1018648.

**Thermal Gravimetric Analysis.**  A TA Instruments TGA Q500 was utilized to parse the thermal stability of the compound and quantify the hydration states and overall water content. This was achieved by loading approximately 15-20 mg of each sample into an alumina pan and heating under a stream of air from 25-1000 °C increasing with a ramp rate of 2 °C/min.  The full TGA data can be found in the supporting information section.

**Vibrational Spectroscopy.**  The presence of solvated water and ligated citrate complexation of the metal center was confirmed with two vibrational spectroscopy techniques.  Each solid compound was pressed into a translucent pellet with KBr as the binder and data was collected on a Nicolet FTIR Spectrometer from 500-4000 cm$^{-1}$.  High Resolution Raman Spectroscopy of a single crystal samples was performed on a Nicolet Almega XR High Performance Dispersive Spectrometer equipped with a 785 nm excitation laser.

**Mass Spectroscopy.** A ThermoElectron LCQ Deca Quadrupole Ion-Trap Mass Spectrometer equipped with an ESI source was used to observe and characterize the existence of the clusters' anionic core in solution. The spectrometer was operated in the negative ion mode and analyzed the samples via direct infusion at a flow rate of 20 uL min$^{-1}$ into the ESI source with a Hamiltonian 250 uL glass syringe. Resultant spectra are an average of approximately 50 scan, collected with a count time of 0.2 s/scan, and nitrogen was employed as the nebulizing gas. Programmable ESI parameters were set as follows: capillary voltage, -16 V; capillary temperature, 110 °C; ionization spray voltage, 3.5 kV; tube lens offset voltage, 20 V. Crystals were dissolved in aqueous solutions, and fragmentation of the anionic species was investigated by varying the pH of the ammonium hydroxide buffer between 4.1 and 10.0 pH.

## Acknowledgments

REFERENCES

1.　K. H. Tan, in *Interactions of Soil Minerals with Natural and Microbes*, eds. P. M. Huang and M. Schnitzer, Soil Science Society of America, Madision, WI, 1986, vol. 17, pp. 1-27.

2.　Y. Hashimoto, *App. Geochem.*, 2007, **22**, 2861-2871.

3.　J. Gerke, W. Romer and A. Jungk, *Z Pflanzenernaehr Bodenkd*, 1994, **157**, 289–294.

4.　P. R. Ryan, R. A. James, C. Weligama, E. Delhaize, A. Rattey, D. C. Lewis, W. D. Bovill, G. McDonald, T. M. Rathjen, E. Wang, N. A. Fettell and A. E. Richardson, *Physio. Plant.*, 2014, **ASAP**.

5.　B. Dinkelaker, V. Romheld and H. Marschner, *Plant . Cell Env.*, 1989, **12**, 285-292.

6.　P. Castaldi, M. Silvetti, E. Mele, G. Garau and S. Delana, *J. Env. Qual.*, 2013, **42**, 774-781.

7.　S. A. Wasay, S. Barrington and S. Tokunaga, *Water, Air, and Soil Pollut.*, 2001, **127**, 301-314.

8.　C. J. Dodge and A. J. Francis, *Environ. Sci. Technol.*, 1994, **28**, 1300-1306.

9.　A. Addelouas, *Elements*, 2006, **2**, 335-341.

10.　P. C. Burns and R. Finch, eds., *Uranium: Mineralogy, Geochemistry, and the Environment.*, Mineralogical Society of America, Washington D.C., 1999.

11.　W. J. Deutsch, K. J. Cantrell, K. M. Krupka, M. L. Lindberg and R. J. Serne, *App. Geochem.*, 2011, **26**, 1681-1693.

12.　J. M. Zachara, P. E. Long, J. Bargar, J. A. Davis, P. Fox, J. K. Fredrickson, M. D. Freshley, A. E. Konopka, C. X. Liu, J. P. McKinley, M. L. Rockhold, K. H. Williams and S. B. Yabusaki, *J. Contam. Hydrol.*, 2013, **147**, 45-72.

13.　K. Maher, J. R. Bargar and G. E. Brown, *Inorg. Chem.*, 2013, **52**, 3510-3532.

14.　S. P. Pasilis and J. E. Pemberton, *Inorg. Chem.*, 2003, **42**, 6793-6800.

15.　K. S. Rajan and A. E. Martell, *Inorg. Chem.*, 1965, **4**, 462-464.

16.　P. G. Allen, D. K. Shuh, J. J. Bucher, N. M. Edelstein, T. Reich, M. A. Denecke and H. Nitsche, *Inorg. Chem.*, 1996, **35**, 784-788.

17.　M. T. Nunes and V. M. S. Gil, *Inorg. Chem. Acta*, 1987, **129**, 283-287.

18.　J. C. Lozano, P. B. Rodriguez, F. V. Tome and C. P. Calvo, *J. Hazard. Mater.*, 2011, **198**, 224-231.

19.　S. D. Ebbs, D. Brady, J. and L. V. Kochian, *J. Exp. Bot..*, 1998, **49**, 1183-1190.

20.　P. Vukosav, M. Mlakar and V. Tomisic, *Anal. Chim. Acta*, 2012, **745**, 85-91.

21.　J. I. Mujika, J. M. Ugalde and X. Lopez, *Phys. Chem. Chem. Phys.*, 2012, **14**, 12465-12475.

22. L. O. Ohman, *Inorg. Chem.*, 1988, **27**, 2565-2570.

23. C. J. Dodge and A. J. Francis, *Environ. Sci. Technol.*, 2002, **36**, 2094-2100.

24. G. L. Booman and W. B. Holbrook, *Analyt. Chem.*, 1959, **31**, 11-16.

25. W. S. Luo and B. H. Gu, *Environ. Sci. Technol.*, 2011, **45**, 2994-2999.

26. B. A. Logue, R. W. Smith and J. C. Westall, *Environ. Sci. Technol.*, 2004, **38**, 3752-3759.

27. G. Redden, J. C. Li and J. Leckie, in *Adsorption of Metals by Geomedia.*, ed. E. A. Jenne, Academic Press, San Diego, CA, 1998, pp. 291-315.

28. C. J. Dodge and A. J. Francis, *Radiochimica Acta*, 2003, **91**, 525-532.

29. C. J. Dodge and A. J. Francis, *Environ. Sci. Technol.*, 1997, **31**, 3062-3067.

30. J. Cejka, in *Uranium: Mineralogy, Geochemistry, and the Environment*, eds. P. C. Burns and R. J. Finch, Mineralogical Society of America, Washington D.C., 1999, vol. 38, pp. 521-622.

31. V. Moulin, J. Tits and G. Ouzounian, *Radiochim. Acta*, 1992, **58/69**, 179-190.

32. J. Baltrusaitis, J. Schuttlefield, E. Zeitler and V. H. Grassian, *Chem. Eng. J.*, 2011, **170**, 471-481.

33. C. Nguyen-Trung, G. M. Begun and D. A. Palmer, *Inorg. Chem.*, 1992, **31**, 5280-5287.

34. S. Fortier and T. W. Hayton, *Coord. Chem. Rev.*, 2010, **254**, 197-214.

35. L. A. Paim, D. V. Augusti, I. Dalmazio, T. M. A. Alves, R. Augusti and H. G. L. Siebald, *Polyhedron*, 2005, **24**, 1153-1159.

36. E. C. Constable, N. Hostettler, C. E. Housecroft, N. S. Murray, J. Schoenle, U. Soydaner, R. M. Walliser and J. A. Zampese, *Dalton Trans.*, 2013, **42**, 4970-4977.

37. K. E. Knope and L. Soderholm, *Chem. Rev.*, 2013, **113**, 944-994.

38. J.-P. Jolivet, C. Chaneac, D. Chiche, S. Cassaignon, O. Durupthy and J. Hernandez, *Comptes Rend. Geosci.*, 2011, **343**, 113-122.

39. C. F. Baes and R. E. Mesmer, *The Hydrolysis of Cations.*, John Wiley and Sons, New York, NY, 1976.

40. D. A. Palmer and C. Nguyen-Trung, *J. Solut. Chem.*, 1995, **24**, 1281-1291.

41. V. Eliet, G. Bidoglio, N. Omenetto, L. Parma and I. Grenthe, *J. Chem. Soc.-Faraday Trans.*, 1995, **91**, 2275-2285.

42. D. L. Clark, S. D. Conradson, R. J. Donohoe, D. W. Keogh, D. E. Morris, P. D. Palmer, R. D. Rogers and C. D. Tait, *Inorg. Chem.*, 1999, **38**, 1456-1466.

43. M. Aberg, *Acta Chem. Scand. A –Phys. Inorg. Chem.*, 1978, **32**, 101-107.

44. C. E. Rowland and C. L. Cahill, *Inorg. Chem.*, 2010, **49**, 8668-8673.

45.    D. Sun, N. Zhang, Q.-J. Xu, R.-B. Huang and L.-S. Zheng, *Inorg. Chem. Comm.*, 2010, **13**, 859-862.

46.    D. K. Unruh, K. Gojdas, E. Flores, A. Libo and T. Z. Forbes, *Inorg. Chem.*, 2013, **52**, 10191-10198.

47.    S. Tsushima, A. Rossberg, A. Ikeda, K. Mueller and A. C. Scheinost, *Inorg. Chem.*, 2007, **46**, 10819-10826.

48.    C. E. Rowland and C. L. Cahill, *Inorg. Chem.*, 2010, **49**, 6716-6724.

49.    E. H. Bailey, J. F. W. Mosselmans and P. F. Schofield, *Chem. Geo.*, 2005, **216**, 1-16.

50.    S. Berto, F. Crea, P. G. Daniele, C. De Stefano, E. Prenesti and S. Sammartano, *Radiochim. Acta*, 2012, **100**, 13-28.

51.    S. L. Heath and A. K. Powell, *Angew. Chem. Int. Ed.*, 1992, **31**, 191-193.

52.    A. K. Powell, S. L. Heath, D. Gatteschi, L. Pardi, R. Sessoli, G. Spina, F. Del Giallo and F. Pieralli, *J. Am. Chem. Soc.*, 1995, **117**, 2491-2502.

53.    A. M. Ako, V. Mereacre, Y. H. Lan, W. Wernsdorfer, R. Clerac, C. E. Anson and A. K. Powell, *Inorg. Chem.*, 2010, **49**, 1-3.

54.    A. M. Ako, O. Waldmann, V. Mereacre, F. Klower, I. J. Hewitt, C. E. Anson, H. U. Gudel and A. K. Powell, *Inorganic Chemistry*, 2007, **46**, 756-766.

55.    M. Murugesu, R. Clerac, W. Wernsdorfer, C. E. Anson and A. K. Powell, *Angew. Chem.-Int. Ed.*, 2005, **44**, 6678-6682.

56.    I. Shweky, A. Bino, D. P. Goldberg and S. J. Lippard, *Inorg. Chem.*, 1994, **33**, 5161-5162.

57.    A. Bino, I. Shweky, S. Cohen, E. R. Bauminger and S. J. Lippard, *Inorg. Chem.*, 1998, **37**, 5168-5172.

58.    A. Peukert and A. Seubert, *J. Chromatogr. A*, 2009, **1216**, 7946-7949.

59.    A.J. Francis, C. J. Dodge, and J.B. Gillow, *Nature*, 1992, **356**, 140-142.

60.    R. W. W. Hoft, *COLLECT*, (1998), Delft, The Netherlands.

61.    G. M. Sheldrick, *APEX II*, (1996) Bruker AXS, Madison, WI.

62.    G. M. Sheldrick, *Acta Cryst. A: Found. .Cryst.*, 2008, **64**, 112-122.

**TABLES**

**Table 1.** Average atom-atom distances obtained from single-crystal X-ray diffraction for the ternary clusters $([(UO_2)_2Fe_4(OH)_4(C_6H_4O_7)_4]^{8-}$ (**U₂Fe₄**), $[(UO_2)_2Fe_2(C_6H_4O_7)_4]^{6-}$ (**U₂Fe₂-1** )and $[(UO_2)_2Fe_2(C_6H_4O_7)_4(H_2O)_2]^{6-}$ (**U₂Fe₂-2**) and $[(UO_2)_2Al_2(C_6H_4O_7)_4]^{6-}$ (**U₂Al₂-1** and **U₂Al₂-2**)) compared to the previously reported values determined by EXAFS spectroscopy by Dodge and Francis[28] for a solid and solution phase with U:Fe:cit ratio of 1:1:2.

| Average Atom-Atom Distances | U₂Fe₄ | U₂Fe₂-1 | U₂Fe₂-2 | U₂Al₂-1 | U₂Al₂ -2 |
|---|---|---|---|---|---|
| **Single-Crystal X-ray Diffraction** | | | | | |
| Metal-O Distance (Å) | 2.014 | 1.985 | 1.995 | 1.876 | 1.874 |
| U-O$_{ax}$ Distance (Å) | 1.79(5) | 1.767(4) | 1.762(4) | 1.772(3) | 1.763(5) |
| U-O$_{eq}$ Distances (Å) | 2.359 | 2.477 | 2.479 | 2.475 | 2.459 |
| Metal-C Distance (Å) | 2.859, 3.081 | 2.74(1) 2.96(8) 3.33(4) | 2.78(2) 2.99(3) 3.322(1) | 2.67(2) 2.86(4) 3.26(2) | 2.66(2) 2.85(4) 3.26(4) |
| Metal-Metal Distance (Å) | 3.037. 3.602 | - | - | - | - |
| Metal-U Distance (Å) | 3.422 3.390 | 3.55(4) | 3.53(1) | 3.46(1) | 3.45(2) |
| **EXAFS (Dodge & Francis, 2003)** | Solid | Aq (15 mM) | | | |
| Metal-O Distance (Å) | 1.99 | 1.98 | | | |
| U-Oax Distance (Å) | 1.77 | 1.77 | | | |
| U-Oeq Distances (Å) | 2.36 | 2.37 | | | |
| Fe- Na Distance (Å) | 2.72 | 2.64 | | | |
| Metal-C Distance (Å) | 3.02 | 3.03 | | | |
| Fe-Fe Distance (Å) | 3.74 | 3.61 | | | |

22

**Table 2.** Selected crystallographic information for $(C_4H_{12}N_2)_3[(UO_2)_2Al_2(C_6H_4O_7)_4](H_2O)_8$ (**U$_2$Al$_2$-1**), $Sr_2(C_2H_{10}N_2)[(UO_2)_2Al_2(C_6H_4O_7)_4](H_2O)_{13}$ (**U$_2$Al$_2$-2**) $(Mg(H_2O)_4)(C_4H_{12}N_2)_2[(UO_2)_2Fe_2(C_6H_4O_7)_4]$ $(H_2O)_7$ (**U$_2$Fe$_2$-1**), $(C_4H_{12}N_2)_3[(UO_2)_2Fe_2(C_6H_4O_7)_4(H_2O)_2](H_2O)_2$ (**U$_2$Fe$_2$ -2**), and $(C_2H_{10}N_2)_4[(UO_2)_2Fe_4(C_6H_4O_7)_4O_2(OH)_4](H_2O)_{14}$ (**U$_2$Fe$_4$**).

| | U$_2$Al$_2$-1 | U$_2$Al$_2$-2 | U$_2$Fe$_2$-1 | U$_2$Fe$_2$-2 | U$_2$Fe$_4$ |
|---|---|---|---|---|---|
| FW (g mol$^{-1}$) | 1754.98 | 1791.75 | 1792.84 | 1740.66 | 2112.53 |
| Space group | $P2_1/n$ | $P$-1 | $P$-1 | $P$-1 | $P$-1 |
| $a$ (Å) | 9.4451(10) | 8.7930(8) | 9.2106(6) | 8.1422(13) | 11.2951(8) |
| $b$ (Å) | 30.530(3) | 10.6713(9) | 9.8799(7) | 11.376(2) | 11.6508(9) |
| $c$ (Å) | 9.7188(11) | 14.5554(13) | 15.1866(10) | 14.798(3) | 14.0541(11) |
| $\alpha$ (°) | 90 | 78.605(3) | 84.120(2) | 84.551(6) | 77.664(3) |
| $\beta$ (°) | 95.311(3) | 85.842(3) | 88.101(2) | 89.290(6) | 71.186(3) |
| $\gamma$ (°) | 90 | 86.569(3) | 83.115(2) | 77.814(6) | 66.255(2) |
| $V$ (Å$^3$) | 2790.4(5) | 1333.9(2) | 1364.49(16) | 1333.7(4) | 1595.0(2) |
| Z | 2 | 1 | 1 | 1 | 1 |
| $\rho_{calc}$ (mg m$^{-3}$) | 2.089 | 2.231 | 2.182 | 2.167 | 2.199 |
| $\mu$ (mm$^{-1}$) | 5.944 | 8.192 | 6.568 | 6.697 | 6.071 |
| F (000) | 1712 | 842 | 864 | 842 | 1036 |
| Crystal Size (mm) | 0.120 x 0.060 x 0.010 | 0.060 x 0.060 x 0.040 | 0.120 x 0.080 x 0.060 | 0.200 x 0.040 x 0.005 | 0.180 x 0.170 x 0.020 |
| Theta Range (°) | 2.544 to 27.463 | 1.430 to 25.379 | 1.348 to 27.105 | 2.900 to 25.097 | 1.538 to 25.014 |
| Data Collected | -12 < $h$ < 12 <br> -39 < $k$ < 39 <br> -12 < $l$ < 12 | -10 < $h$ < 10 <br> -12 < $k$ < 12 <br> -17 < $l$ < 17 | -11 < $h$ < 11 <br> -12 < $k$ < 12 <br> -19 < $l$ < 19 | -9 < $h$ < 9 <br> -13 < $k$ < 13 <br> -17 < $l$ < 17 | -13 < $h$ < 13 <br> -12 < $k$ < 13 <br> -16 < $l$ < 16 |
| Reflections Collected/ Unique | 55 350/6364 [R$_{int}$ = 0.0550] | 20 450/4864 [R$_{int}$ = 0.0470] | 23 483/6002 [R$_{int}$ = 0.0245] | 23 431/4725 [R$_{int}$ = 0.0660] | 18 604/5575 [R$_{int}$ = 0.0550] |
| GOF of F$^2$ | 1.055 | 1.08 | 1.067 | 1.013 | 1.102 |
| Final $R$ Indices [I > 2σ(I)] | $R_1$ = 0.0252 <br> w$R_2$ = 0.0480 | $R_1$ = 0.0417 <br> w$R_2$ = 0.1104 | $R_1$ = 0.0346 <br> w$R_2$ = 0.0795 | $R_1$ = 0.0353 <br> w$R_2$ = 0.0644 | $R_1$ = 0.0385 <br> w$R_2$ = 0.0948 |
| $R$ Indices (all data) | $R_1$ = 0.0396 <br> w$R_2$ = 0.0524 | $R_1$ = 0.0502 <br> w$R_2$ = 0.1166 | $R_1$ = 0.0429 <br> w$R_2$ = 0.0836 | $R_1$ = 0.0580 <br> w$R_2$ = 0.0715 | $R_1$ = 0.0453 <br> w$R_2$ = 0.0981 |

**FIGURE CAPTIONS**

**Figure 1.** Polyhedral units of **U$_2$Al$_2$** representing the heterometallic molecular core composed of two central uranyl cations and two exterior aluminum cations linked via tetradentate chelation of four citrate ligands. The yellow and blue polyhedra correspond to the U(VI) and Al(III) cations and the black and red spheres are C and O atoms, respectively.

**Figure 2.** Polyhedral representations of **U$_2$Fe$_2$-1** (a) and **U$_2$Fe$_2$-2** (b) are composed of two central uranyl hexagonal bipyramids and two exterior ferric octahedral chelated by four citrate molecules. The yellow and brown polyhedra denote the U(VI) and Fe(III) cations and the black and red spheres are C and O atoms, respectively. Major differences between the two species are highlighted by the green circle, showing additional water molecules complexed to the Fe(III) polyhedra and the unbound carboxylate arm of the citrate molecule in **U$_2$Fe$_2$-2**.

**Figure 3.** **U$_2$Fe$_4$** contains four central Fe(III) cations and two outer $UO_2^{2+}$ cations that are chelated by four citrate ligands in a tetradentate coordination to form the $[(UO_2)_2Fe_4(C_6H_4O_7)_4O_2(OH)_4]^{8-}$ cluster. The yellow and brown polyhedra denote the $U(VI)O_2^{2+}$ and Fe(III) cations and the black and red spheres are C and O atoms, respectively.

**Figure 4.** The infrared spectra for **U$_2$Fe$_4$**, **U$_2$Fe$_2$**, and **U$_2$Al$_2$** indicate the presence of ligated and solvated water constituents in the crystalline material and confirm the citrate ligand is complexed to the metal center.

**Figure 5.** The Raman spectra for **U$_2$Fe$_4$**, **U$_2$Fe$_2$**, and **U$_2$Al$_2$** reveals the red shifted $\nu_1$ symmetric stretch associated with the uranyl moiety that corresponds to complexation of the citrate molecule and formation of polynuclear ternary species.
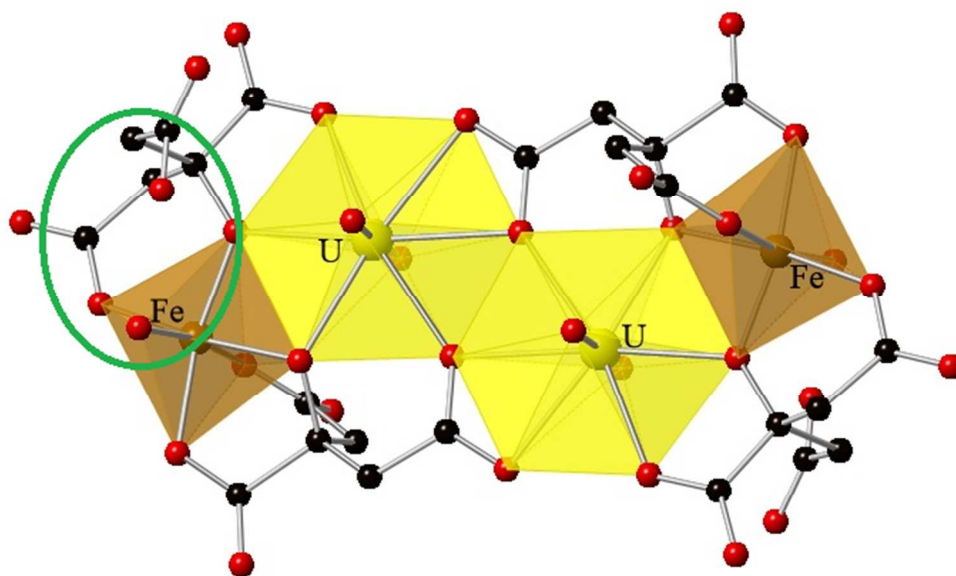
**TOC graphic**
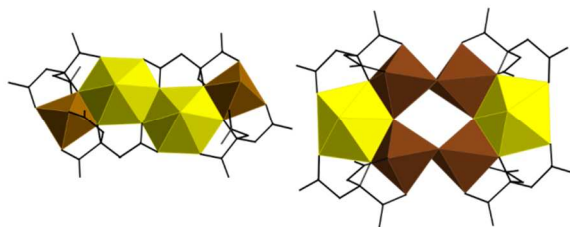


Structural characterization of U(VI):(Al(III), Fe(III)):citrate complexes provides insight into the formation of polynuclear clusters present in environmentally-relevant aqueous solutions.
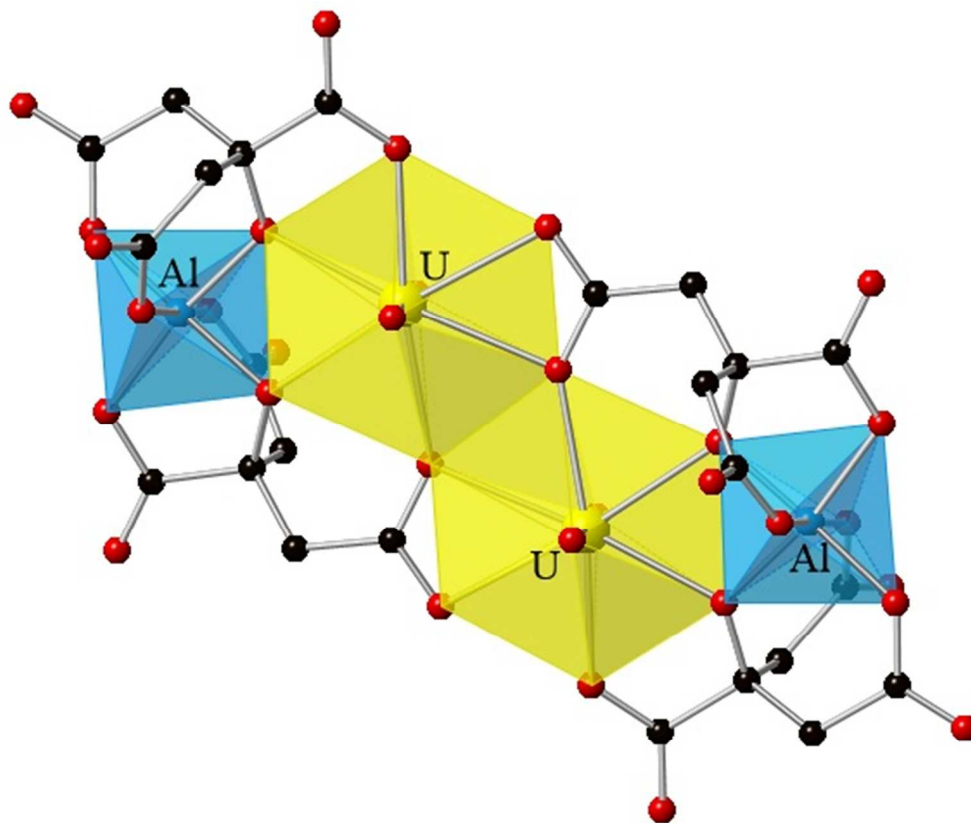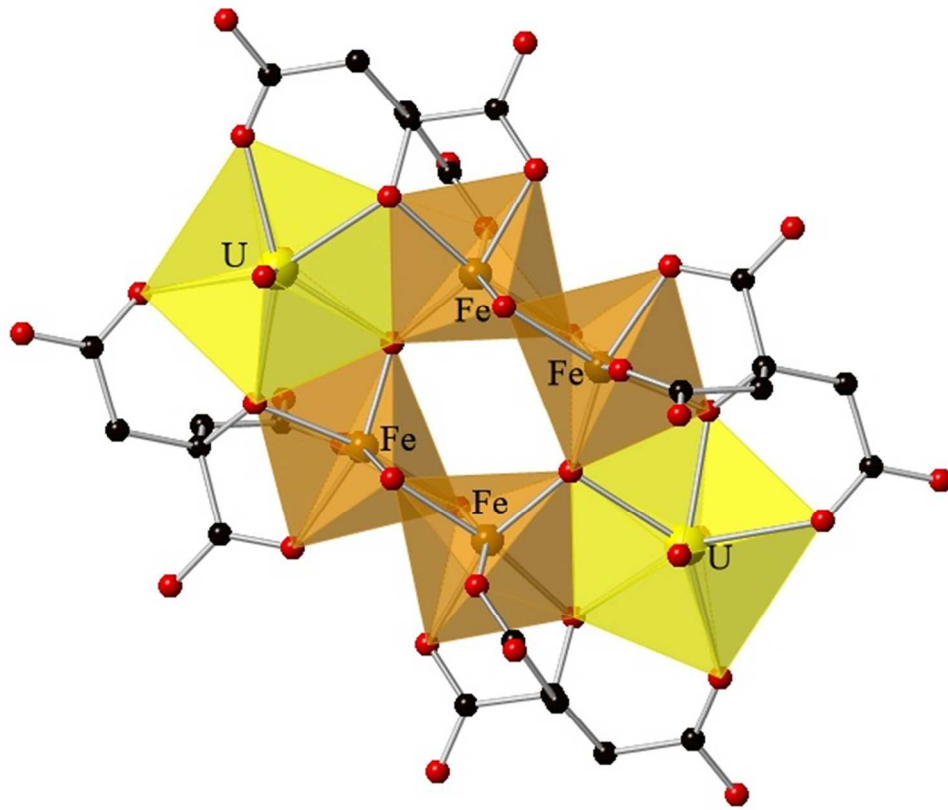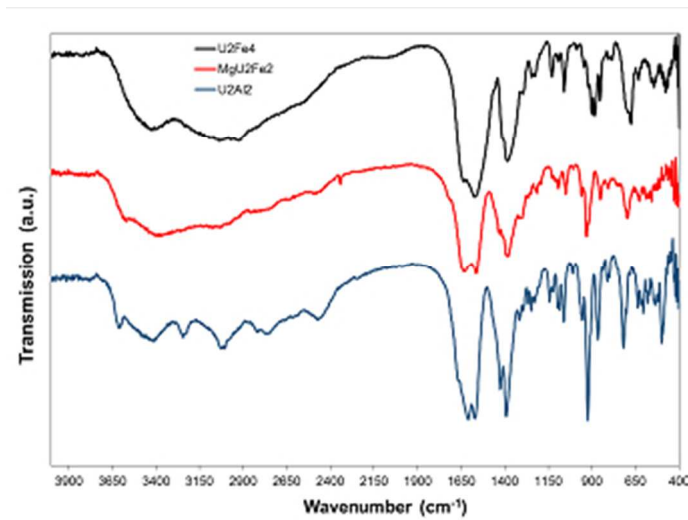
153x129mm (96 x 96 DPI)
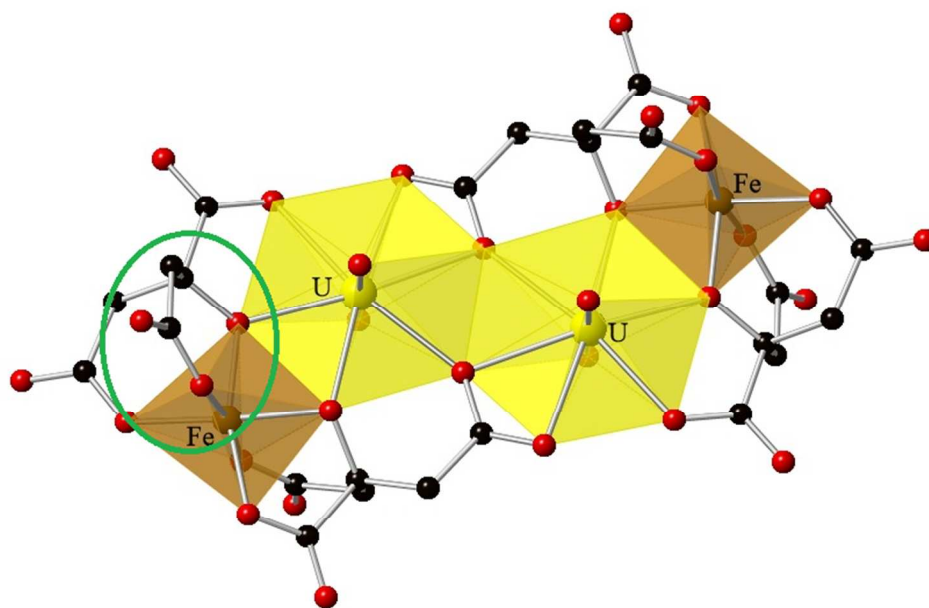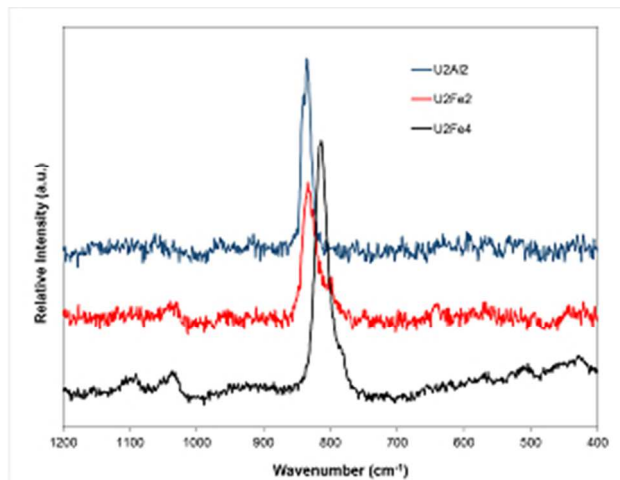
227x143mm (96 x 96 DPI)

186x110mm (96 x 96 DPI)

175x144mm (96 x 96 DPI)

89x68mm (96 x 96 DPI)

81x63mm (96 x 96 DPI)